Development of robust light-weight deformable mirrors in carbon fiber

Michael Hart, Logan Richardson
Steward Observatory, University of Arizona, Tucson, AZ 85721, U.S.A.

Robert Romeo, Robert Martin
Composite Mirror Applications Inc., 1638 Research Loop, Tucson, AZ, USA 85710, U.S.A.

ABSTRACT

Carbon fiber reinforced polymer (CFRP) has recently been developed to the point that surfaces of high optical quality can be routinely replicated. Building on this advance, we are developing a new generation of deformable mirrors (DMs) for adaptive optics application that extends long-standing expertise at the University of Arizona in large, optically powered DMs for astronomy. Our existing mirrors, up to 90 cm in diameter and with aspheric deformable face sheets, are deployed on a number of large astronomical telescopes. With actuator stroke of up to 50 microns and no hysteresis, they are delivering the best imaging ever seen from an astronomical AO system. Their Zerodur glass ceramic face sheets though are not well suited to non-astronomical applications. In this paper, we describe developmental work to replace the glass components of the DMs with CFRP, an attractive material for optics fabrication because of its high stiffness-to-weight ratio, strength, and very low coefficient of thermal expansion. Surface roughness arising from fiber print-through in the CFRP face sheets is low, < 3 nm PTV across a range of temperature, and the optical figure after correction of static terms by the DM actuators is on the order of 20 nm rms. After initial investment in an optical quality mandrel, replication costs of identical units in CFRP are very low, making the technology ideal for rapid mass production.

Keywords: Adaptive optics, deformable mirrors

1. INTRODUCTION AND MOTIVATION

A significant breakthrough in astronomical adaptive optics (AO) was achieved a decade ago when the first adaptive secondary mirror (ASM) was installed on the 6.5 m MMT telescope on Mt. Hopkins, AZ.[1] For the first time, AO was included as an integral part of the telescope rather than being added in a down-stream instrument. This realized a number of advantages important to astronomical science; in particular, by removing many optical surfaces from the beam train, the optical throughput of the AO-corrected telescope was improved, and the thermal emissivity of the whole system was dramatically reduced, giving the MMT a critical edge at wavelengths longward of 2.5 μm. The mirror, shown in Figure 1, required a number of technology advances, including the manufacture of large, thin, curved face sheets in glass without compromising the accuracy of the aspheric optical figure demanded of a telescope's mirrors. Large stroke was assured by use of voice coil actuators, with collocated capacitive sensors to provide highly accurate position control with no hysteresis. A sophisticated control system was developed to drive the mirror and maintain dynamic stability at kilohertz update rates.[2]

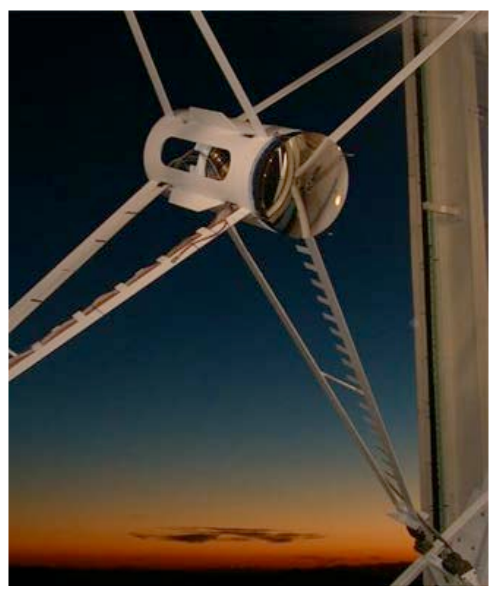

Figure 1. The world's first adaptive secondary mirror, installed at the 6.5 m MMT telescope in southern Arizona. The mirror is 64 cm in diameter.

Now, we foresee that other applications besides astronomy will benefit from deformable mirrors with similar properties: large, optically powered and with actuators of high stroke and fast response time. But while the ASMs developed for astronomy have demonstrated excellent performance in the field, there are applications for which the Zerodur face sheets may not be well suited. These are generally cases in which the ASM may experience large accelerations or be handled with less than ideal care by non-experts. For this reason we are developing a new generation of DM which maintains the desirable features of the ASMs while replacing the fragile face sheet and heavy backing structure with carbon fiber reinforced polymer (CFRP) as a robust lightweight substitute.[3,4] CFRP is a suitable material for optical fabrication because of its low weight-to-stiffness ratio (five times less than steel), a coefficient of thermal expansion (CTE) that can be tuned to near-zero with specialized carbon layup arrangements, and good thermal conductivity.[4] CFRP mirrors are now free of fiber and core print-through issues and demonstrate excellent adhesion between optical coatings and the polymer surface. Because they are made by replication from a durable mandrel, Figure 2, the cost of mass production is low. In addition, CFRP and Zerodur have similar Young's moduli, but because CFRP is much tougher, it may be made into thinner face sheets which require substantially less power to be driven into a given desired shape, since the stiffness of a sheet scales as the cube of its thickness.

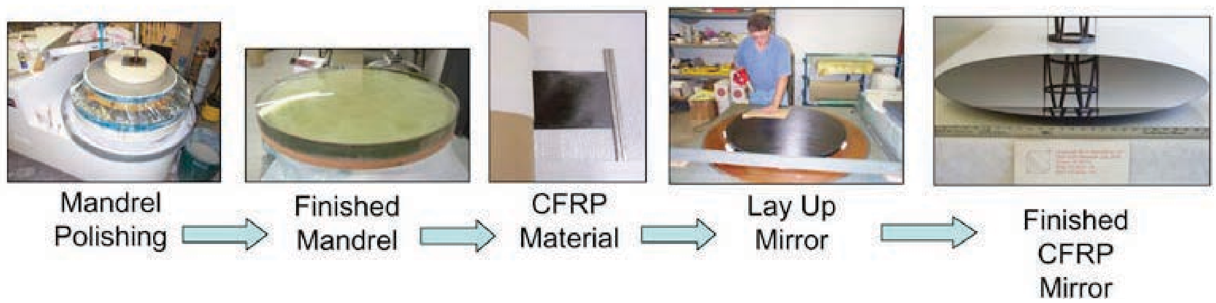

Figure 2. The manufacturing process for CFRP mirrors begins with a polished glass mandrel having the shape of the finished mirror but with opposite curvature. CFRP material is laid over the mandrel which is then treated with a proprietary process to produce the final face sheet.

2. ASTRONOMICAL TECHNOLOGY HERITAGE

The AO system built around the first ASM at the MMT has been very successful scientifically. It has also led directly to the development of a second generation of ASMs at the twin 8.4 m Large Binocular Telescope (LBT), shown in Figure 3, on Mt. Graham, AZ and one of the 6.5 m Magellan telescopes in Chile.[5] The two mirrors on the LBT are 91 cm in diameter, with concave ellipsoidal surfaces to implement a Gregorian configuration for the telescope. The Zerodur face sheets are on average just 1.7 mm thick; there is some variation with radius because the back surfaces are spherical.

The LBT is now producing the highest quality images from any astronomical AO system, with Strehl ratios >80% in the astronomical H band around 1.6 μm wavelength.[6] An early example from 2010 is shown in Figure 4. In part the excellent performance of the LBT's AO is attributable to the optical quality of the DM face sheet and the precise

LBT adaptive secondary mirrors

Diameter:	91 cm
Actuator count:	672
Response time:	0.5 ms
Stroke:	50 μm
Surface (rms):	15 nm
Figure:	Concave ellipsoid

Figure 3. The Large Binocular Telescope on Mt. Graham, Arizona has two 8.4 m primary mirrors on a common mount. Both sides of the telescope feature an adaptive secondary mirror.

position control of the actuators. The voice coil actuators exhibit no hysteresis, since the capacitive sensors controlling the position respond purely monotonically. Furthermore, since they make no physical connection between the face sheet and the structures behind it, the high quality optical surface is not disturbed by manufacturing errors in the actuators, and should one fail, the optical surface is not pinned but floats freely under the influence of its neighbors. This avoids the introduction of wave front errors of high spatial frequency which scatter light broadly across the field.

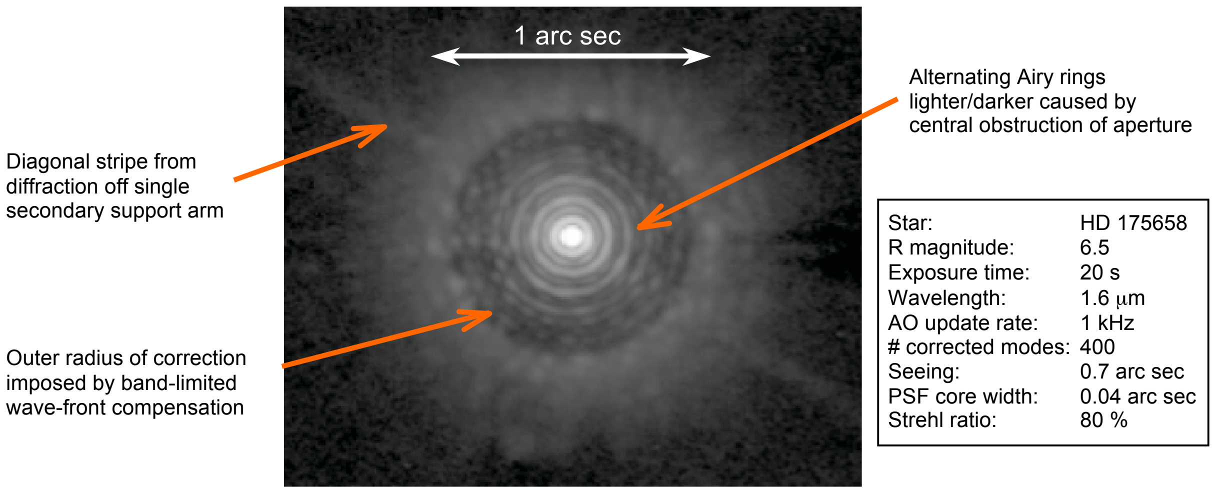

Figure 4. Stellar image recorded with one half of the LBT with the telescope's ASM running at 1 kHz. The Strehl ratio achieved by the correction on this 8.4 m aperture is 80% at 1.6 μm wavelength. The image is shown on a logarithmic gray scale with the core saturated to highlight the details of the PSF. (Image courtesy S. Esposito and the LBT First Light AO team of the Arcetri Observatory, Florence.)

3. PROTOTYPE 17 cm CFRP DEFORMABLE MIRROR

The new mirrors in CFRP will maintain the desirable qualities that have made the astronomical ASMs so successful, but at the same time will be much more robust, much lighter in weight, and will operate with reduced power consumption in worse turbulence. The carbon fiber components of these mirrors are manufactured by Composite Mirror Applications (Tucson, AZ). To date, a series of face sheets of 8 cm and 17 cm diameter have been made, with thickness of 1.4 mm. The figure in each case is a concave sphere. Very recently, a light-weight CFRP reaction body, just 100 g, has also been fabricated to match the size and curvature of the 17 cm face sheets. Figure 5 shows one of the 17 cm face sheets under investigation in the lab, made from a mandrel with 680 mm radius of curvature, integrated with the reaction body. The reaction body itself is also shown separately with the 19 New Focus picomotor actuators used to change the DM's shape. The mirror is held in place against the picomotors by magnets bonded to the rear surface of the CFRP shell (Figure 6). To thermally decouple the CFRP from the iron magnets, a thin piece of fused silica is inserted between the two, with each interface secured by three small dots of epoxy glue.

A finite element model (FEM) of the reaction body has been developed to understand its behavior in response to actuator forces. An example is shown in Figure 7, where the central actuator is pushed with 0.1 N against balancing forces from the remaining actuators. This is about the largest inter-actuator force that we would expect to need for correction of atmospheric turbulence. The peak deformation of the reaction body is 44 nm. While this is about an order of magnitude lower than the deformation of the face sheet itself, it is not negligible, and so will need to be taken into account in the control law used to drive the DM.

The use of picomotors is intended only as a temporary arrangement, since they are too massive and have a response time orders of magnitude too slow for use in real-world AO applications. They serve to support the face sheet for tests of its opto-mechanical properties, and to explore the thermal behavior, but for final prototyping, they will be replaced by a new generation of linear actuators.[7] These are inspired by the voice coils of the ASMs, but rely on an opposing pair of coils embedded in a soft iron yoke to drive an iron disk placed between the coils. An axial shaft

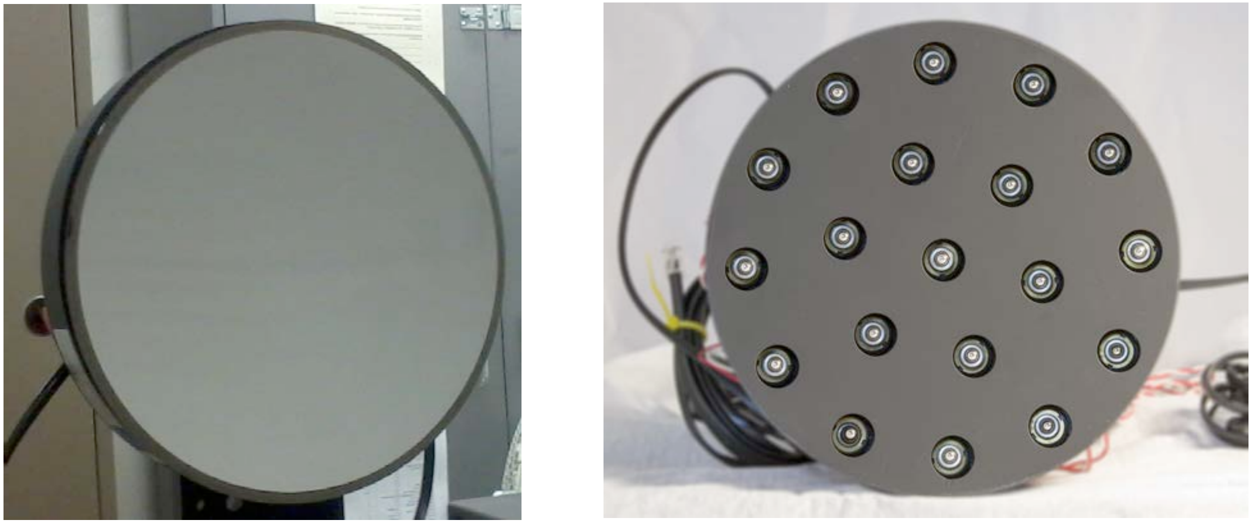

Figure 5. (*Left*) View of a 17 cm CFRP deformable mirror. For initial tests, the reaction body (*right*) is outfitted with 19 New Focus picomotor actuators, which account for 90% of the weight of the assembly. In future, these will be replaced with a new generation of high-efficiency linear actuator.[7] The actuators attach to the rear surface of the face sheet via neodymium magnets.

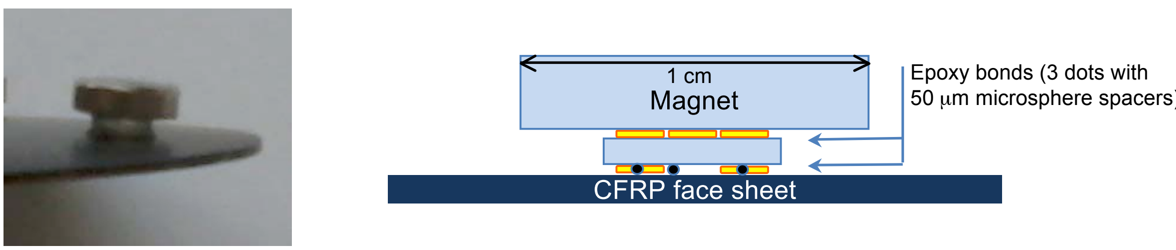

Figure 6. The attachment of the actuator magnets to the rear surface of the CFRP face sheet. The photograph shows one of the magnets bonded to the face sheet in Figure 5. The cartoon illustrates the components in the assembly.

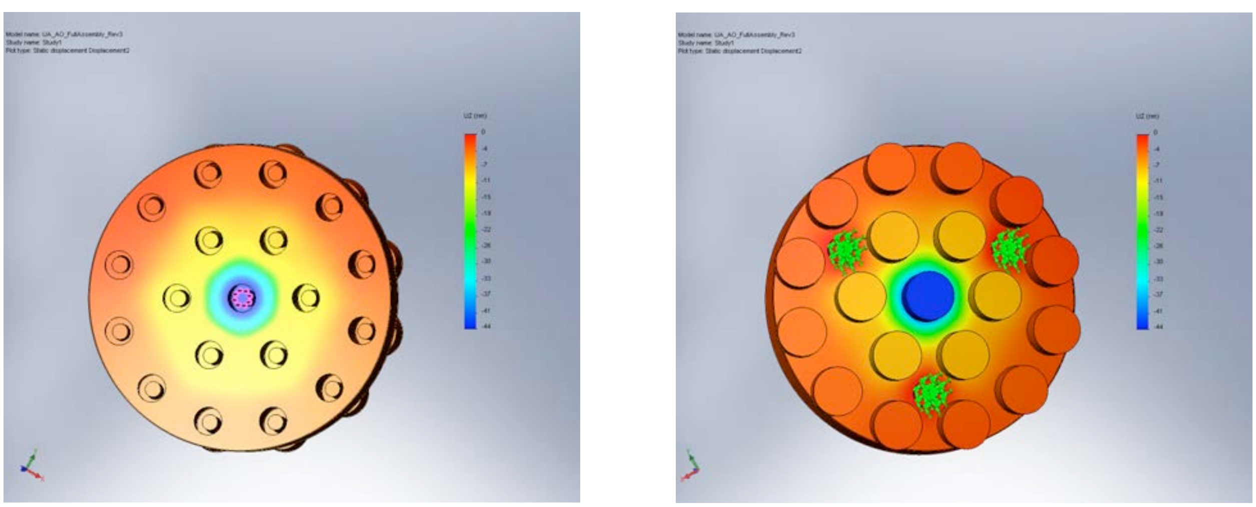

Figure 7. Results from FEM analysis of the CFRP reaction body. The modeled disturbance is a 0.1 N force applied to the central actuator, balanced by opposing forces on the other 18 actuators. This represents the largest forces typically expected for correcting atmospheric turbulence. The maximum deformation is 44 nm.

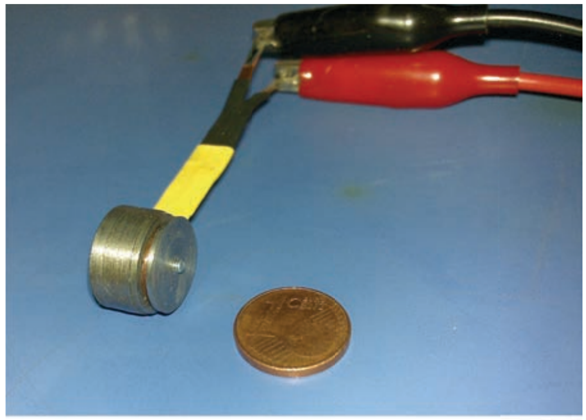

Figure 8. First prototype of the electromagnetic linear actuator that will replace the picomotors in the final CFRP deformable mirrors. (From Del Vecchio et al.)

running through the center of the disk bears on the permanent magnet attached to the back of the face sheet to transmit the motion to the optical surface.

A prototype of the actuator, shown in Figure 8, has demonstrated a critical advantage of this new design over the voice coils: the driving force is directly proportional to the electrical power dissipation, rather than the square root of the power. This makes the actuator fundamentally more efficient. For correction of moderate to poor atmospheric turbulence at an upward-looking ground-based telescope, for example, we estimate that the dissipation will be no more than 0.1 W per actuator, an order of magnitude less than the present ASMs. A further major advantage is that the coaxial capacitive sensor required by the voice coils for real-time position feedback is no longer needed. This is because the reluctance of the magnetic circuit in the actuator is itself a function of the actuator's position, and so the position can be derived directly from a separate circuit in the driver electronics. By eliminating the capacitive sensor, the actuators may be packed on centers of about 12 mm rather than the 30 mm typical of the ASMs, required because of the physical size of the sensor pads. The new DMs will therefore be capable of correcting at substantially higher spatial frequency, easily down to visible wavelengths. But equally significantly, the capacitive sensors are implemented across an air gap of just 70 μm between the back surface of the face sheet and the front surface of the reaction body. This limits the stroke of the ASMs and introduces a vulnerability should dust find its way into the gap. In the new DMs, in contrast, the spacing between face sheet and reaction body can be several millimeters, allowing for larger stroke and more robust operation.

4. OPTICAL AND THERMAL TESTS OF THE FACE SHEETS

Optical figure measurements have been performed with a Twyman-Green 4D interferometer (PhaseCam 4020). The optical quality of one of the 8 cm pieces at room temperature is shown in Figure 9. This mirror had 7 actuators attached to the back surface, a regular hexagon with an additional one in the center. Since the face sheet is entirely unconstrained otherwise, this arrangement allows only four bending modes to be introduced. In its relaxed state, with no actuator forces applied, the aberration was 92 nm rms. After best adjustment of the actuators, the error was reduced to less than 40 nm rms across the entire mirror. Most of the error is attributable to edge curvature, outside the radius addressable by the actuators. The forces required to correct the natural, relaxed shape of the 8 cm CFRP piece are estimated to be ~0.1 N for each actuator. These values are well within the range of the linear actuators described above; the prototype has already demonstrated more than 1 N.

We have found that the optical quality of the face sheets is limited by the mandrel. White light interferometric tests, illustrated in Figure 10, show that the peak-to-valley small scale surface roughness is approximately 3 nm which is sufficiently low for high quality imaging in the visible and near IR wavebands. Measurements across larger patches of the mirror surface indicate that the errors on spatial scales of ~0.5 mm are on the order of 10 nm rms. Although print-through from the fibers is apparent at a very low level in the interferometry, its effect will be rather benign, scattering a small fraction of incident light to large angles. This will lead to a slight reduction in image contrast, but at visible wavelengths, the scattered component will be less than 2%. The resolving power of optical systems based on these DMs will be unaffected.

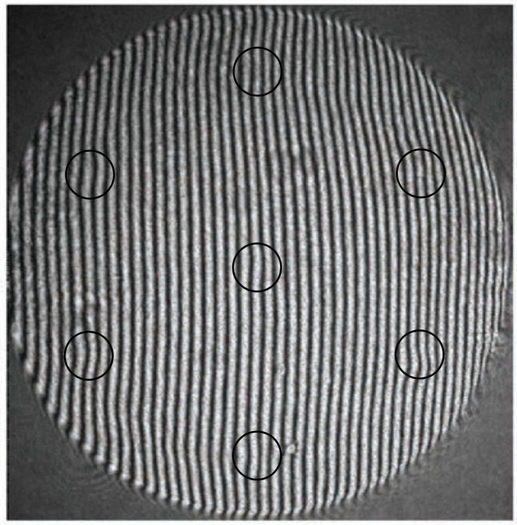

Figure 9. Interferogram of one of the 8 cm CFRP face sheets after best correction by its seven actuators. Minor localized deformation of the surface can be seen at the locations of some of the actuators (marked with circles).

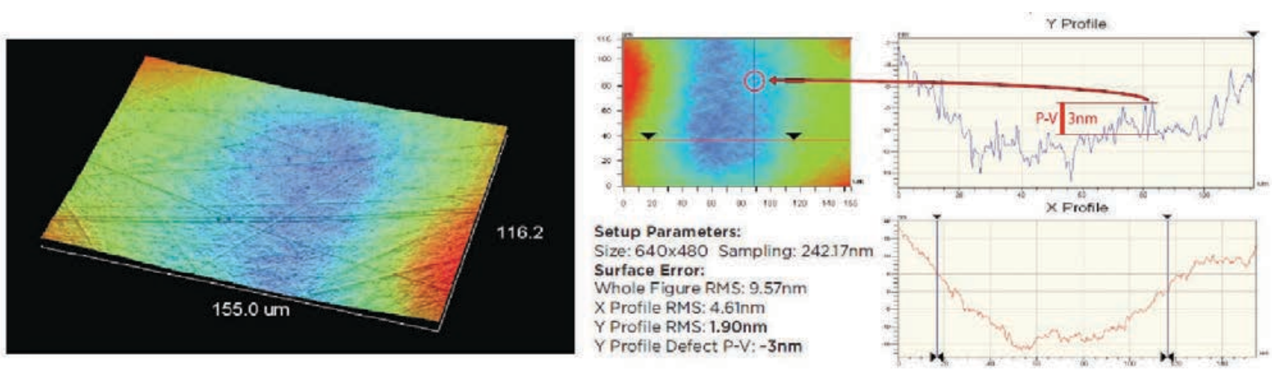

Figure 10. White light interferogram of a 116×155 μm patch of an 8 cm CFRP face sheet. The left and middle panels show the phase as color. Individual fibers are seen in the phase map. The right panels display horizontal and vertical cuts of the phase. The overall shape is the prescribed spherical curvature of the mirror. The surface roughness of the piece due to the carbon fibers is 3 nm P-V.

Early results with the 17 cm DM are shown in Figure 11. Initially, the face sheet has been supported in the reaction body with just three of its 19 actuators to allow the relaxed shape to be measured. The aberration is 180 nm rms. Although that is twice as large as the aberration seen in the 8 cm piece in its relaxed configuration, the magnitude of the increase is actually cause for encouragement rather than concern. The actuators can remove the aberration, at least on spatial scales longer than twice the actuator spacing, but the question is the force required, and the dynamic range lost in doing so. If the mean force per actuator is not to increase, then the error can increase no faster than the square of the mirror diameter. These initial observations therefore suggest that the CFRP manufacturing process will scale readily to mirrors of larger diameter; our goal is eventually to proceed to mirrors of 1 m diameter.

As of this writing, we have not tested the DM with all actuators optimized to produce the lowest residual aberration. We can estimate the value however by applying a high-pass spatial filter that removes power on spatial scales larger than the Nyquist limit of the actuators. That result is also shown in Figure 11. The residual error is clearly dominated by edge curvature outside the influence of the actuators. Over the whole surface, the aberration is reduced to 75 nm rms, and within the radius of actuator control, the error is 46 nm rms. At this level, better than $\lambda/10$, we can be confident that the mirror will deliver good optical quality as part of an AO system.

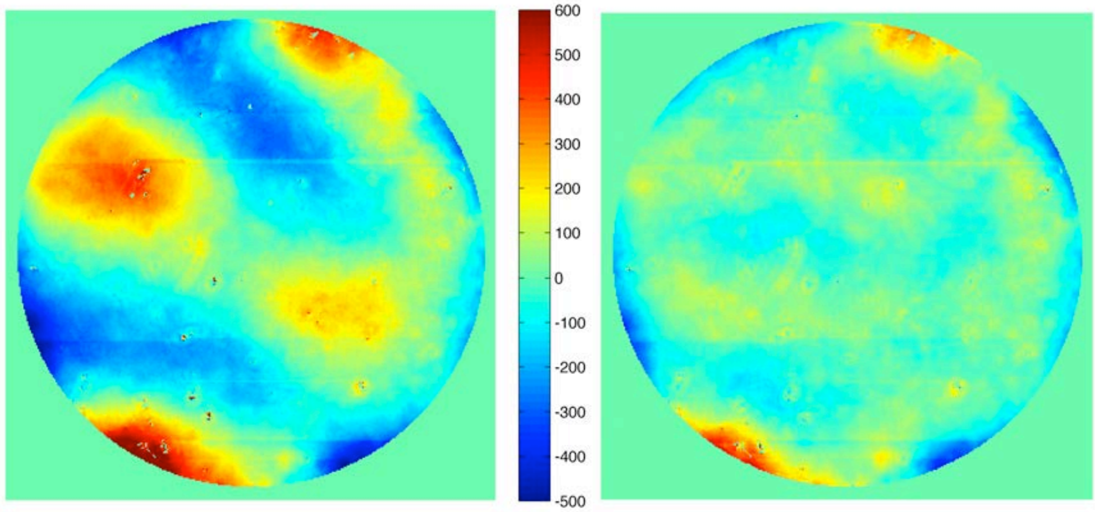

Figure 11. (*Left*) Surface map of a 17 cm face sheet held vertically by just 3 actuators, showing the relaxed shape of the optical surface. The magnitude of the aberration is 1.1 μm peak-to-valley and 180 nm rms. (*Right*) The shape after high-pass spatial filtering to the level expected with 19 actuator control. The scale bar is in nm.

We have begun to test the optical surface quality of the face sheets with temperature by repeating the 4D interferometer measurements of one of the 8 cm mirrors inside a freezer. For these tests, areas of the mirror at the edge and affected by actuator print-through were excluded since we are mainly interested in understanding how thermal effects can be compensated by the control system. The results, summarized in Figure 12, demonstrate that there is indeed some shape change as the temperature drops from 15°C to -7°C. With no changes to the actuator settings, the rms figure error with power removed increases roughly linearly from 17 nm to 40 nm. The residual figure error is reduced to 33 nm by optimizing the actuator control. Nonetheless, over this temperature range, the mirror figure remains acceptable. We have yet to explore performance at higher temperatures, but from symmetry arguments we expect the results to be qualitatively similar.

5. FUTURE WORK AND DISCUSSION

CFRP deformable face sheets have reached a level of maturity that demonstrates high optical quality, with aberrations less than λ/10 after wave front flattening by the DM actuators. With new high-efficiency electromagnetic actuators, and lightweight carbon fiber backing structures, they promise to offer scalable, robust deformable mirrors that do double duty: introducing phase (and, with appropriate optical conjugation, amplitude) compensation, while at the same time applying optical power to either focus or collimate the beam. These mirrors will enable AO for directed energy and fielded imaging systems requiring large stroke and efficient optics. The new materials allow the construction of DMs with less than half the weight of conventional lightweighted glass optics.

A number of outstanding issues remain to be addressed. In the near term, we plan to test the environmental durability of the CFRP material by placing samples at the site of the LBT telescope and subjecting them over periods of months to the same weathering as normal telescope optics. During that time, they will be tested for any changes in optical and mechanical properties. Also of concern is the behavior of the figure error as the mirror increases in size. Provided that this error scales no more sharply than the square of the diameter, then the force required per actuator to correct it does not grow and the error remains correctable. The results from our 8 cm and 17 cm parts are encouraging in this respect, but we intend to explore further, with prototype face sheets up to 50 cm diameter.

For astronomical application, these mirrors have potential value as substitutes for what has over the past decade become the conventional way to make adaptive secondary mirrors. Although glass may be polished to very high optical quality, and there is a deep history and understanding of doing so, there is no escaping the unfortunate combination of facts that large thin glass face sheets are fragile and expensive. In some cases, the superior quality of glass will always be preferred, but the results we have described here show that CFRP deformable mirrors will be a

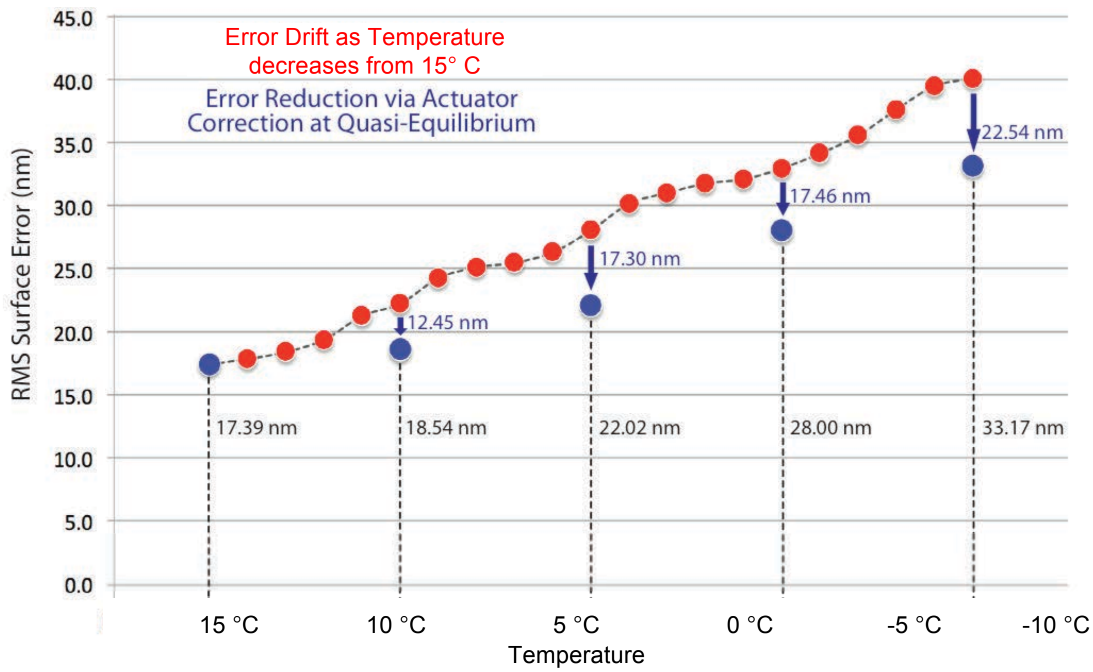

Figure 12. Wave-front error over an 8 cm thin-shell CFRP mirror with tilt and power removed. RMS surface error as a function of temperature.

viable alternative where a modest trade in performance (primarily image contrast) can be made for the sake of cost and robustness. We are now looking at this trade for the case of the Giant Magellan Telescope (GMT),[8] shown in artist's conception in Figure 13. The GMT, to be constructed on Cerro Las Campanas in Chile, is an international partnership to build a 25 m telescope that will synthesize a fast *f*/0.7 primary mirror of 25 m diameter from seven 8.4 m segments. The adaptive optics will rely on a concave Gregorian ASM, segmented in the same way as the primary mirror, with segments of 1.06 m diameter.

Because the outer six segments of the GMT secondary mirror are all off-axis aspheres, there is an added challenge in manufacturing these face sheets, as well as the reaction bodies to support the capacitive sensors, since they too must be aspheric. But because these segments are all characterized by the *same* off-axis asphericity, there is a great potential cost saving to be achieved by adopting CFRP. In that case, only a single off-axis mandrel need be made, from which all six CFRP face sheets would be replicated. Furthermore, even if environmental testing shows that the CFRP face sheets will last only a year or two operating in the open air, it will be a straightforward matter to manufacture spares as needed while still remaining well below the cost envelope of the glass ASMs.

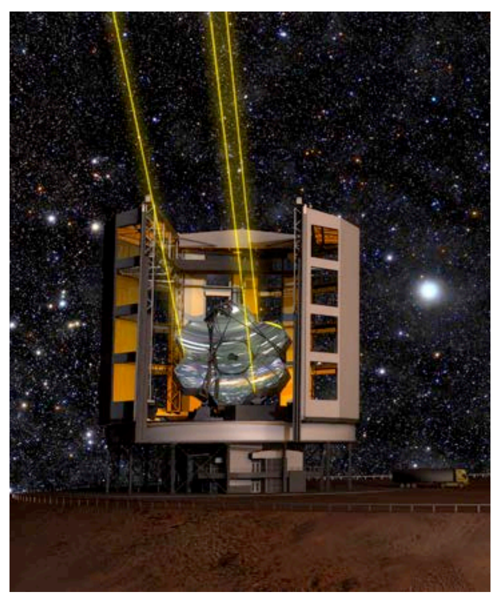

Figure 13. The Giant Magellan Telescope will synthesize a 25 m primary mirror from seven 8.4 m segments. The secondary mirror will be adaptive, with 1 m segments in the same geometry.

ACKNOWLEDGMENTS

This work has been supported in part by the Giant Magellan Telescope Project Office under contract GMT-AO-CON-00285. We are grateful to S. Esposito and C. Del Vecchio of the Osservatorio Astrofisico di Arcetri for valuable discussions.

REFERENCES

[1] Lloyd-Hart, M., Brusa, G., Wildi, F. P., Miller, D. L., Fisher, D. L., and Riccardi, A., "Lessons learned from the first adaptive secondary mirror," in Astronomical Adaptive Optics Systems and Applications, eds. R. K. Tyson and M. Hart, Proc. SPIE **5169**, 79–89 (2003).

[2] Biasi, R., Fini, L., Mantegazza, P., Biliotti, V., Gori, F., and Gallieni, D., "Control electronics for an adaptive secondary mirror," in Adaptive Optical System Technologies, eds. D. Bonaccini and R. K. Tyson, Proc. SPIE **3353**, 1193–1201 (1998).

[3] Ammons, S. M., Hart, M., Coughenour, B., Romeo, R., Martin, R., and Rademacher, M., "Demonstration of 17 cm robust carbon fiber deformable mirror for adaptive optics," in Astronomical Adaptive Optics Systems and Applications IV, eds. R. K. Tyson & M. Hart, Proc. SPIE **8149**, 81490C (2011).

[4] Romeo, R. and Martin, R., "Progress in 1 m-class lightweight CFRP composite mirrors for the ULTRA telescope," in Optomechanical Technologies for Astronomy, Proc. SPIE **6273**, 62730S (2006).

[5] Close, L. M., Gasho, V., Kopon, D., Males, J., Hinz, P., and Hare, T., "The Magellan telescope deformable secondary adaptive optics system," Bulletin of the American Astronomical Society, **41**, 674 (2010).

[6] Esposito, S. et al., "First light AO (FLAO) system for LBT: final integration, acceptance test in Europe, and preliminary on-sky commissioning results," in Adaptive Optics Systems II, eds. B. L. Ellerbroek, M. Hart, N. Hubin, & P. L. Wizinowich, Proc. SPIE **7736**, 773609 (2010).

[7] Del Vecchio, C., Agapito, G., Arcidiacono, C., Carbonaro, L., Marignetti, F., De Santis, E., Biliotti, V., & Riccardi, "The actuator design and the experimental tests of a new technology large deformable mirror for visible wavelengths adaptive optics," in Adaptive Optics Systems III, eds. B. L. Ellerbroek, E. Marchetti, & J.-P. Véran, Proc. SPIE **8447**, (2012).

[8] Shectman, S. and Johns, M., "GMT overview," in Ground-based and Airborne Telescopes III, eds. L. M. Stepp, R. Gilmozzi, & H. J. Hall, Proc. SPIE **7733**, 77331Y (2010).